Geotechnical Engineering, Vol.21, 1990

PASSIVE EARTH PRESSURE OF PARTIALLY SATURATED SOILS

A. Siva Reddy* and Alok Agrawal**

SYNOPSIS

Herein, passive earth resistance in partially saturated soils is analysed by the method of characteristics. The effect of initial suction pressure and Skempton's pore pressure parameters on the failure surfaces and passive resistance is studied. The effect of initial suction on the effective normal pressure along the wall is to increase it and is found to be considerable. Results are presented in the form of passive earth pressure coefficients.

INTRODUCTION

It is well known that vast areas of soils on the surface of the earth are classified as arid or semi arid regions. However, the stability problems related to these partially saturated soils have not received due attention. Many researchers argue that the additional strength imparted to soil due to suction should not be relied upon. Still, worth considering is the question, whether or not it is possible to use this reserve strength to economize the design. Reddy & Mogaliah (1970) used the method of characteristics to find the bearing capacity of such soils. The soil was considered to have an initial non-dimensional negative pore water pressure, u_0/c (where c is cohesion of the soil taken as characteristic stress for non-dimensionalization), which upon loading changes to final non-dimensional pore water pressure, u/c. The expression for u/c was derived using Skempton's (1954) equation to find the change in pore water pressure. Considering the equilibrium of a two dimensional soil element under the action of various stresses, body force and pore water pressure u, the equations along the characteristics were derived.

In the work reported here these equations are used to analyse the passive earth pressure of partially saturated soils against inclined retaining walls with rough surfaces. Results are presented in the form of passive earth pressure

*Professor of Civil Engineering, Indian Institute of Science, Bangalore 560 012, INDIA.

**Research Scholar, Department of Civil Engineering, Indian Institute of Science, Bangalore 560 012, INDIA.

coefficients k_{pc}, k_{pg} and $k_{p\gamma}$. The final negative pore water pressure at the horizontal top of the backfill is taken as positive surcharge in the computations of k_{pg}. Effects of Skempton's pore pressure parameters A and B and u_0/c on normal effective stress on the wall and failure pattern are studied.

ANALYSIS

The schematic diagram of an inclined retaining wall, with horizontal backfill, is shown in Fig. 1. The retaining wall makes an angle β_0 with the vertical. The following assumptions are made:

1. Problem is two-dimensional
2. Soil mass is rigid plastic at failure
3. Soil mass is at failure at each and every point considered
4. The Mohr-Coulomb failure criterion is valid for the soil.

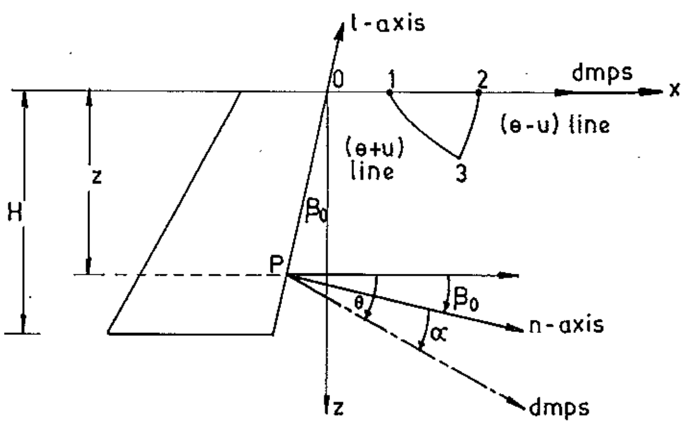

Fig. 1 Definition Sketch

The expression for u at any point as given by Reddy & Mogaliah (1970) is as follows:

$$u = \frac{B}{1-B}\left[\sigma\{1 + (2A-1).\sin\phi\} - H + \gamma z(Ak_0 - k_0 - A) + u_0(k_0-1)(1-A)\right] + \frac{u_0}{B} \quad (1)$$

where

$$\sigma = \frac{\sigma_1 + \sigma_3}{1} + H = \frac{\sigma_x + \sigma_z}{2} + H \text{ (see Figure 2)}$$

z = depth of the point being considered
γ = unit weight of soil
ϕ = angle of internal friction
H = c.cotϕ (see Fig. 2)
k_0 = coefficient of earth pressure at rest
θ = angle between the x-axis and the direction of major principle stress, taken as positive clockwise

From the same paper the following equations along the characteristics are taken

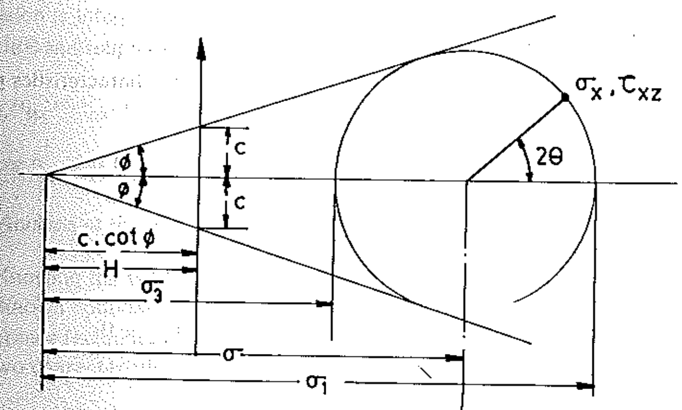

Fig. 2 Mohr's circle of stress

$$\frac{dz}{dx} = \tan(\theta \pm \mu) \quad (2)$$

and

$[1 + M \pm M.\tan\phi.\cot(\theta \pm \mu)].d\sigma \pm 2\bar{\sigma}.\tan\phi.d\theta \pm M.\tan\phi\,[\tan(\theta \pm \mu) + \cot(\theta \pm \mu)].$

$$\frac{\partial \sigma}{\partial x}.dx = \pm \frac{N.\cos(\theta \pm \mu)}{\cos\phi.\cos(\theta \pm \mu)} .dx \qquad (3)$$

where, $M = \frac{B}{1-B}[1(2A-1).\sin\phi]$, $N = \gamma.[1 - \frac{B}{1-B}(Ak_0 - A - k_0)]$ and

$$\mu = 45 - \phi/2.$$

The equations corresponding to the upper sign hold along the $(\theta + \mu)$ characteristic while those corresponding to the lower sign hold along the $(\theta - \mu)$ characteristics.

The normal stress components in x and z directions σ_x and σ_z, respectively, and the shear stress t_{xz} at any point can be represented in terms of σ and θ as,

$$\left.\begin{matrix}\sigma_x\\ \sigma_z\end{matrix}\right\} = \sigma(1 \pm \sin\phi.\cos 2\theta) - H \qquad (4)$$

$$T_{xz} = \sigma \sin\phi.\sin 2\theta \qquad (5)$$

Finite difference techniques are used for the integration of equations 2 and 3 to arrive at the values of σ and θ at various points on the characteristics grid points.

a) Boundary Conditions

i) Along ox

Fig. 1 shows the direction of malor principal stress along

ox. As $\tau_{xz} = 0$ along $z = 0$, we have from equation 5, $\theta_{ox} = 0$ (6)

From equation 1, u at $z = 0$ is given as

$$u_{z=0} = U1\sigma - H.U2 + U3 \qquad (7)$$

where

$$U2 = \frac{B}{1-B}$$

$$U1 = U2[1 + (2A-1).\sin\phi$$

$$U3 = [U2.(k_0 - 1).(1-A) + 1/(1-B)]\, u_0$$

Let q be any normal surcharge acting along ox. The vertical effective stress along ox, $\sigma'_{z(ox)} = 0 - u_{z=0}$.

Therefore from equations 4, 6 and 7, the following expression for o along ox, σ'_{ox} is obtained

$$\sigma'_{ox} = \frac{q + (1 + U2).H - U3}{1 - \sin\phi + U1} \qquad (8)$$

ii) At the singular point '0'

Here, at the same point '0' the value of θ is different at the right of '0' from that at the left of it. Also, here the $(\theta-\mu)$ line shrinks to a point. To obtain a closed form solution in terms of σ and θ at this point, $dx = 0$ and $dz = 0$ are substituted in the equation along the $(\theta-\mu)$ characteristic. The resulting expression is integrated and the constant of integration is evaluated by using the conditions given by equations 7 and 8.

$$\sigma_{sp} = \sigma'_{ox}.\exp[2\tan\phi(\theta_{sp} - \theta_{ox})/(1 + M)] \qquad (9)$$

where σ_{sp} and θ_{sp} are the values of σ and θ, respectively at the singular point.

iii) Analysis at the intersection of two characteristics

Knowing the values x, z, σ and θ at points 1 and 2 (see Fig. 1), which lie on the known boundary, equations 2 and 3 are integrated numerically by the finite difference technique to obtain the values of these parameters at the intersection of two characteristics.

Writing equations 2 in the finite difference form and solving for x_3 and z_3 (i.e., for the co-ordinates of the point of intersection of the two characteristics)

$$x_3 = \frac{(z_2 - z_1) + x_1.\tan(\theta_1 - \mu) - x_2.\tan(\theta_2 + \mu)}{\tan(\theta_1 - \mu) - \tan(\theta_2 + \mu)} \qquad (10)$$

and

$$z_3 = z_1 + (x_3 - x_2).\tan(\theta_1 - \mu) \qquad (11)$$

The equation along the $(\theta - \mu)$ characteristic is written in the finite difference form as follows

$$[1 + M - M.\tan\phi.\cot(\theta_2 - \mu)].(\sigma_3 - \sigma_2) - 2\sigma_2\tan\phi\,(\theta_3 - \theta_2) + M\tan\phi$$
$$[\tan(\theta_2 - \mu) + \cot(\theta_2 - \mu)]\ \frac{\partial\sigma_2}{\partial x_2}(x_3 - x_2) = -\frac{N.\cos(\theta_2 + \mu)}{\cos\theta.\cos(\theta_2 - \mu)}(x_3 - x_2) \quad (12)$$

Defining the following

$$A1 = 1 + M - M.\tan\phi.\cot(\theta_2 - \mu),\ A2 = 2\sigma_2\tan\phi$$

$$A3 = M.\tan\phi\,[\tan(\theta_2 - \mu) + \cot(\theta_2 - \mu)]\ \frac{\partial\sigma_2}{\partial x_2}(x_3 - x_2)$$

$$A4 = \frac{N.\cos(\theta_2 + \mu)}{\cos\phi.\cos(\theta_2 - \mu)}(x_3 - x_2),$$ and solving for σ_3

$$\sigma_3 = \frac{A1.\sigma_2 + A2\,(\theta_3 - \mu_2) - A3 - A4}{A1} \quad (13)$$

Similarly, from the equation along the $(\theta - \mu)$ characteristic the following expression for σ_3 can be obtained

$$\sigma_3 = \frac{B1\,\sigma_1 - B2\,(\theta_3 - \theta_1) + B3 + B4}{B1} \quad (14)$$

where

$$B1 = 1 + M + M\tan\phi\,\cot(\theta_1 + \mu),$$

$$B2 = 2\sigma_1\tan\phi$$

$$B3 = M\tan\phi[\tan(\theta_1 + \mu) + \cot(\theta_1 + \mu)]\ \frac{\partial\sigma_1}{\partial x_1}(x_3 - x_1)$$

$$B4 = \frac{N.\cos(\theta_1 - \mu)}{\cos\phi.\cos(\theta_1 + \mu)}(x_3 - x_1)$$

Equating the equation 13 and 14 and solving for θ_3

$$\theta_3 = \frac{AB3}{A1.B2 + B1.A2} \quad (15)$$

where

$$AB1 = A1.B1.(\sigma_1 - \sigma_2) + A1.(B3 + B4)$$

$$AB2 = B1\,(A3 + A4) + A2.B1.\theta_2 + A1.B2.\theta_1$$
$$AB3 = AB1 + AB2$$

Therefore, having calculated the co-ordinates of the point of intersection of the two characteristics from equations 10 and 11, θ_3 is computed from equation 15 and thereafter σ_3 from either of the equations 13 and 14. The values of σ and θ at points 1 and 2 are then averaged with their values at point 3 to obtain a new estimate of σ_1, θ_1 and σ_2, θ_2. The calculations of σ_3 and θ_3 are then repeated.

iv) Analysis along the wall

Considering the state of stress at any point P on the wall the value of θ along the wall, θ_w, is obtained. Choosing n and t axes as shown in Fig. 1, the shear stress τ_{nt} on the soil element P at the point of incipient failure is given by

$$\tau_{nt} + (c.\cot\phi + \sigma_n).\tan\delta$$

where σ_n is normal stress on wall and δ is angle of wall friction. This relation can be expressed as (see Fig. 2)

$$\sigma.\sin\phi.\sin 2\alpha = +[c.\cot\phi + \sigma\{1 + \sin\phi.\cos 2\alpha\} - c.\cot\phi]\tan\delta$$

where $\alpha = \theta_w - \beta_o$

$$\text{whence } \theta_w = \beta_o + \frac{\delta}{2} + \frac{1}{2}.\sin^{-1}(\sin\delta/\sin\phi) \quad (16)$$

The expression for the normal stress at the wall, σ_n, is given by

$$\sigma_n = \sigma(1 + \sin\phi.\cos 2\alpha) - c.\cot\phi \quad (17)$$

where α is as shown in Fig. 1.

b) Computation of Coefficients of Passive Earth Pressure

Let the normal component of passive earth pressure at any point P at a depth z below 0 be P_{pn}. It is given by equations 17 and is expressed in terms of earth pressure coefficients as

$$P_{pn} = c.k_{pc} + \gamma\,z.k_{p\gamma}\,q.k_{pq}$$

where k_{pc}, k_{pq} and $k_{p\gamma}$ = non-dimensional passive earth pressure coefficients due to c, γ and q, respectively.

Firstly the σ_n at P on the wall due to cohesion only (i.e., P_{pc}) is obtained taking soil weight and surcharge as zero in a dry soil.

Therefore,

$$k_{pc} = P_{pc}/c \tag{19}$$

In the second run a positive surcharge, q, equal to the final negative pore water pressure, which can be calculated from the equation 7 and 8, is assumed to act along ox. Taking the soil to be weightless and in a dry state the normal pressure P_{pcq} due to surcharge and cohesion is obtained at the point P. k_{pg} is calculated using

$$k_{pq} = (P_{pcq} - ck_{pc}/q \tag{20}$$

In the third run the non-dimensional normal passive pressure P_{pn}, for partially saturated soil considering both weight and surcharge is computed. $k_{p\gamma}$ is calculated from

$$k_{p\gamma} = \frac{P_{pn} - c.k_{pc} - q.k_{pg}}{\gamma z} \tag{21}$$

where, q = −u at z = o which can be obtained from equation 7.

First, the slip line field is generated in all these three runs to calculate the normal pressure at different points along the wall. This pressure is again determined at the predetermined points by linear interpolation. At these points k_{pc}, k_{pq} and $k_{p\gamma}$ are calculated.

NON−DIMENSIONALIZATION

All the equations are non-dimensionalized by dividing the stresses by the characteristic stress and by dividing the linear dimensions by the characteristic length. In this paper the non-dimensional variables are represented by adding prime to dimensional variables. Defining c = characteristic stress and $l = c/\gamma$ = characteristic length, the non-dimensional form of equations 1, 4 to 15 and 17 to 21 are

$$u/c = \frac{b}{(1-A)} [\sigma' [1 + (2A-1)\sin\phi] - \cot\phi +$$

$$z' (Ak_0 - A - k_0 + u_0/c(k_0 - 1)\ (1-A) + \frac{u_0/c}{B}\ ] \tag{22}$$

u_0/c and u/c = non-dimensional pore water pressures.

$$\left.\begin{matrix}\sigma_x' \\ \sigma_z'\end{matrix}\right\} = \sigma'(1 \pm \sin\phi.\cos 2\theta) - \cot\phi \tag{23}$$

$$\tau'_{xz} = \sigma' \sin\phi.\sin 2\theta \tag{24}$$

$$u/c_{z=o} = U1\ \sigma' - \cot\phi\ U2 + U3 \tag{25}$$

$$\sigma'_{ox} = [\ q' + (1 + U2).\cot\phi - U3\ ] \ / \ (1 - \sin\theta + U1\ ) \tag{26}$$

$$\sigma'_{sp} = \sigma'_{ox} \exp\ [2\tan\phi\ (\varnothing_{sp} - \theta_{ox}) / \ (1 + M)] \tag{27}$$

$$x_3' = \frac{(z_2' - z_1') + x_1' \tan(\theta_1 - \mu) - x_2 \tan(\theta_2 + \mu)}{\tan(\theta_1 - \mu) - \tan(\theta_2 + \mu)} \tag{28}$$

$$z_3' = z_1 + (x_3 - x_1) \tan(\theta_1 - \mu) \tag{29}$$

$$\sigma_3' = \frac{A1 \sigma_2' + A2' (\theta_3 - \theta_2) - A3' - A4'}{A1} \tag{30}$$

$$= \frac{B1 \sigma_1' - B2' (\theta_3 - \theta_1) + B3' + B4'}{B1} \tag{31}$$

where

$$A4' = \frac{N'.\cos(\theta_2 + \mu)}{\cos\phi.\cos(\theta_2 - \mu)} (x_3' - x_2') \text{ and } B4' = \frac{N'\cos(\theta_1 - \mu)}{\cos\phi.\cos(\theta_1 + \mu)} (x_3' - x_1') \tag{32}$$

$$N' = 1 - \frac{B}{1-B} (Ak_0 - A - k_0) \tag{33}$$

$$A3' = M\tan\phi[\tan(\theta_2 - \mu) + \cot(\theta_2 - \mu)]\ \frac{\partial \sigma_2'}{\partial x_2'}\ (x_3' - x_2') \tag{34}$$

$$B3' = M\tan\phi[\tan(\theta_1 + \mu) + \cot(\theta_1 + \mu)] \frac{\partial \sigma_1'}{\partial x'_1} (x'_3 - x'_1) \tag{35}$$

$$A2' = 2\sigma'_2 \tan\phi \tag{36}$$

$$B2' = 2\sigma'_1 \tan\phi \tag{37}$$

and

$$\theta_3 = \frac{AB3'}{A1\,B2' + B1.A2'}$$

where

$$AB1' = A1\,B1(\sigma_1 - \sigma_2) + A1(B3' + B4')$$

$$AB2' = B1\,(A3' + A4') + A2'\,B1.\,\theta_2 + A1\,B2'.\,\theta_1 \text{ and } AB3' = AB1' + AB2' \tag{38}$$

$$\sigma'_n = \sigma'\,(1 + \sin\phi.\cos 2\alpha) - \cot\phi \tag{39}$$

$$P'_{pn} = k_{pc} + z'\,k_{p\gamma} + q'k_{pq} \tag{40}$$

where, $q' = -u/c$ at $z' = o$

$k_{pc} = P'_{pc}$, $k_{pq} = (P'_{pq} - k_{pc})/q'$

and

$$k_{p\gamma} = \frac{P'_{pn} - k_{pc} - q'k_{pq}}{z'} \tag{41}$$

Using the non-dimensional equations, the characteristic grid is generated. The procedure was programmed and performed on a computer.

RESULTS AND DISCUSSION

As already explained the passive earth pressure against the retaining wall has been expressed in terms of k_{pc}, k_{pq} and $k_{p\gamma}$. Knowing these factors at any point z below the top. and having calculated $q = -u/c_{z=0}$ from equation 25, P_{pn} can be obtained. Numerical results for different values of A, B, u_0/c, ϕ, δ and β_0 are presented. The value of k_0 throughout the analysis had been taken as 0.6.

i) Failure Pattern

Figs. 3 and 4 show the failure patterns for different values of the parameters. It can be seen that with increasing values of initial suction the failure

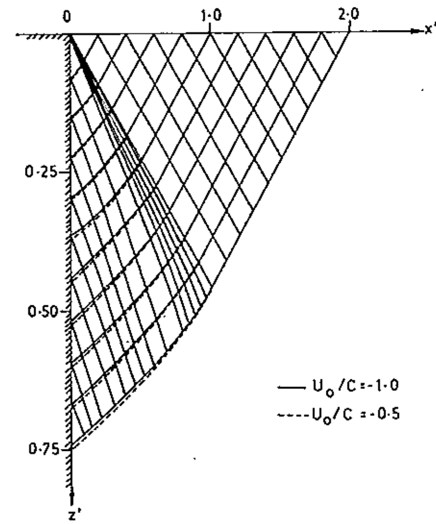

Fig. 3 Failure contours for A = B = 0.2, ϕ = 40°, δ = 10° and β_0 = 0°

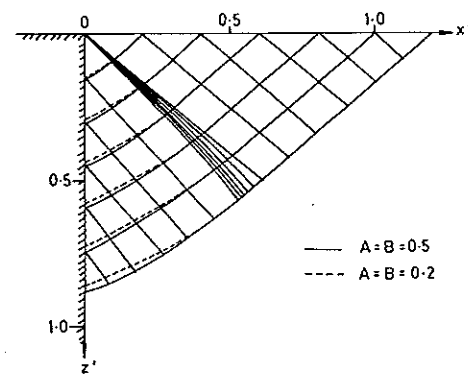

Fig. 4 Failure pattern for ϕ = 10°, δ = 2.5°, u_0/c = −0.5 and β_0 = 0°

planes become shallower. Contrary to this, with the increasing level of saturation (i.e., greater values of A and B), at constant initial negative pore water pressure, the failure planes go deeper. Also the effect of change in the failure surfaces is more pronounced. It can also be seen that in Rankine's passive zone the failure planes remain the same for both the cases.

ii) Comparison with the results for dry soil

Taking A, B and u_0/c equal to zero in the analysis, values for the dry soil are obtained. These values are compared for a case of A = B = 0.2 and u_0/c = − 0.5 and − 1.0 in Figs. 5 and 6. It is seen that with increasing initial suction the non-dimensional normal pressure along the wall, σ_n', increases due to an enhanced level of shear strength of the soil. The increase in σ_n' due to increase in suction pressure from zero at the dry state to −1.0 at unsaturated state, at any depth, is as much as about 30%.

iii) Influence of various parameters on σ_n and earth pressure coefficients

It has been found that the values of k_{pc} and k_{pq} remain constant throughout the depth of the retaining wall. k_{pq} had been noted in the figures for different cases. k_{pc} depends on the values of ϕ δ and β_0 only. Table 1 gives values of k_{pc} for the various cases considered in the paper. k_{pq} is also a function of the surcharge q', which in turn, depends upon the values of A, B u_0/c, σ_{ox}' and k_0. Therefore, for every set of values of A, B u_0/c and k_0, there will be different values of σ_{ox}' and q' and hence of k_{pq}. $k_{p\gamma}$, on the other hand, has been found to vary with depth.

Figs. 7 and 8 show the effect of u_0/c on k_p , k_{pq} and σ_n'. It can be inferred that as u_0/c decreases from −0.5 to −1.0, σ_n' and k_{pq} increase. Figs. 9 and 10 show the $k_{p\gamma}$ distribution and values of k_{pc} and k_{pq} for an inclined retaining wall. Figs. 11 and 12 show the effect of increasing value of parameter B on k_{pq} and $k_{p\gamma}$. It can be seen that both k_{pq} and $k_{p\gamma}$ decrease due to increase in the value of B. It is to be expected that the shear strength of soil decrease at an enhanced level of saturation, therefore resulting in decreased values of σ_n' along the wall. Figs. 13 and 14 show the distribution of u/c along the wall. The final pore water pressure can be seen to be increasing along the wall with depth. It is also seen that the increase in the final pore water pressure is approximately of the same order as the change in the inital suction. Knowing the value of σ' at any point on the back of the wall the final pore water pressure can be calculated from equation 1.

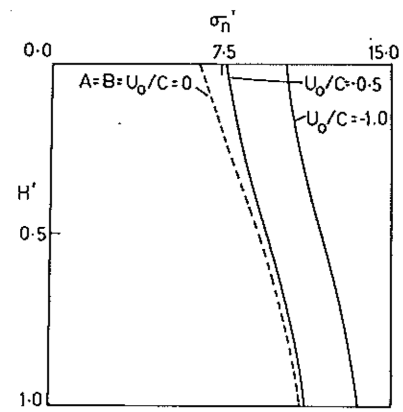

Fig. 5 Non-dimensional normal pressure, σ_n', distribution for A = B = 0.2, ϕ = 40°, δ = 0.25 and β_0 = 0° (shown by solid line)

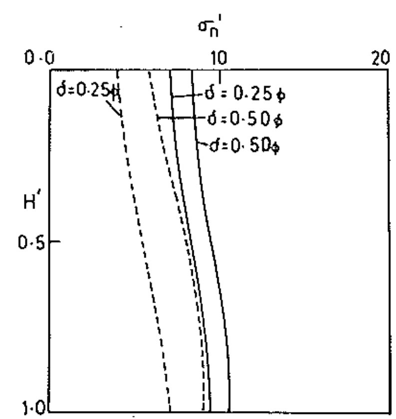

Fig. 6 Non-dimensional pressure, σ_n', distribution for, β_0 = 0°, ϕ = 30°, A = B = 0.2, and u_0/c = −1.0 (shown by solid line)

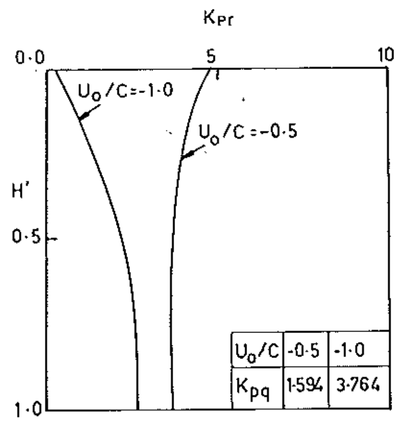

Fig. 7 $k_{p\gamma}$ **for A = B = 0.2, β_0 = 10°, ϕ = 30° and δ = 7.5°**

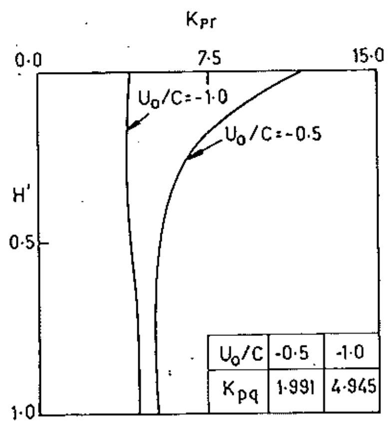

Fig. 8 $k_{p\gamma}$ **for A = B = 0.2, β_0 = 0°, ϕ = 40° and δ = 10°**

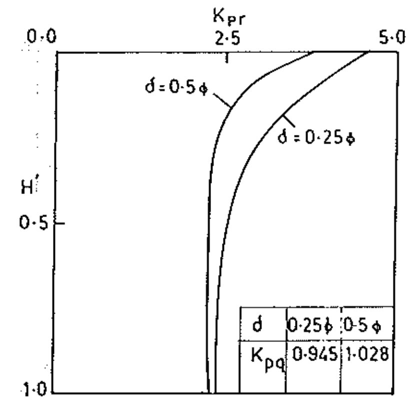

Fig. 9 $k_{p\gamma}$ **for A = B = 0.2, ϕ = 20°, u_0/c = −0.5 and β_0 = 5°**

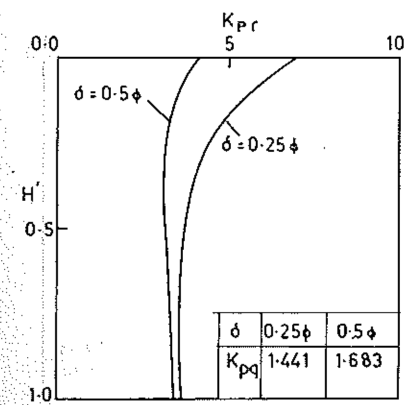

Fig. 10 $k_{p\gamma}$ **for A = B = 0.2, ϕ = 30°, u_0/c = −0.5 and β_0 = 5°**

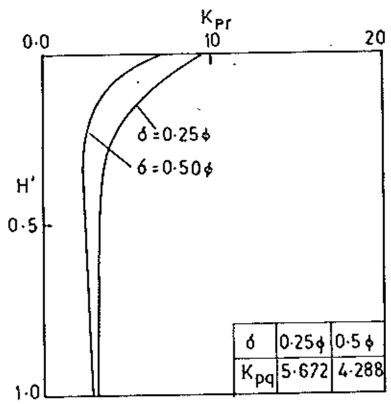

Fig. 11 $k_{p\gamma}$ for A = B = 0.2, β_0 = 0°, u_0/c = 1.0 and ϕ = 30°

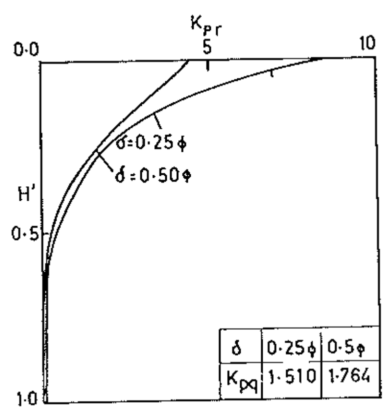

Fig. 12 $k_{p\gamma}$ for A = 0.2, B = 0.5, β_0 = 0°, u_0/c = −1.0 and ϕ = 30°

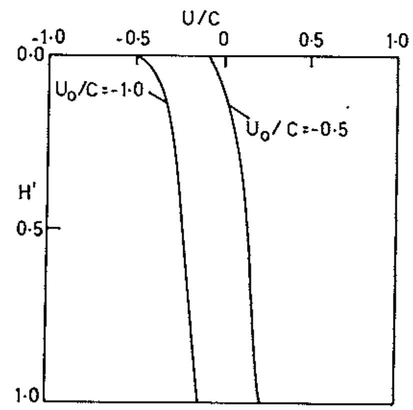

Fig. 13 Distribution of non-dimensional final pore water pressure, u/c, along the wall for A = B = 0.2, ϕ = 40°, β_0 = 0° and δ = 10°

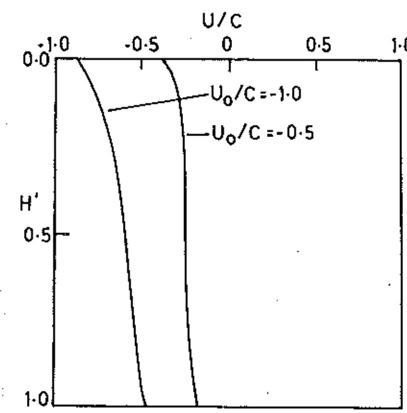

Fig. 14 Distribution of non-dimensional pore water pressure along the wall for A = B = 0.2, o = 10°, β_0 = 0° and δ = 2.5°

CONCLUSIONS

The analysis and the results presented give the influences of the pore wat pressure parameters A and B and u_0/c on the failure surfaces. With an increa of A and B the failure planes to deeper. With an increase of initial suction th become shallower. An increase in the values of A and B reduces the norn effective stress along the wall because of an enhanced degree of saturation constant pore water pressure. Also, everything else remaining constant, great values of initial suction (i.e., lesser u_0/c) result in higher values of norn effective stress along the wall because of improved shear strength.

Table 1. Values of k_{pc} for different ϕ, δ and β_0

β_0	ϕ	k_{pc} for δ =		
		0.25ϕ	0.5ϕ	0.75ϕ
	10°	2.762	3.061	3.275
0°	30°	4.627	5.694	6.540
	40°	6.482	8.793	5.590
5°	20°	3.920	4.504	4.937
	30°	5.301	6.479	7.410
10°	30°	6.044	7.347	8.376

REFERENCES

REDDY, A.S. & MOGALIAH, G. (1970). "Bearing capacity of partially saturated soi *Journal of Soil Mechanics and Foundation Engineering, ASCE*, Vol.96, No. SM6, 2175–2180.

SKEMPTON, A.W. (1954). "The pore pressure coefficients A and B". *Geotechnic* Vol.IV, pp. 145–147.